THE FUNCTION AND REGULATION OF KYNURENINE PATHWAY INTERMEDIATES IN BREAST CANCER METABOLISM

By

TAYAH SOMMER

A thesis submitted in fulfillment of the requirements for the
Honours Program in the Department of Biology

This Advanced Research Project has been accepted by:

Chair, Department of Biology

Dean of Science

Department of Biology
University of Prince Edward Island
Charlottetown, Prince Edward Island

May, 2023

ABSTRACT

Breast cancer (BC) is the second leading cause of cancer related deaths in Canadian women, making it an important area for research. Most cancer cells require an altered metabolism making them vulnerable to metabolism-based therapies. Among metabolic pathways, the kynurenine pathway (KP) of *de-novo* NAD+ biosynthesis contains several intermediates, which have been shown to have a bioactive role in immune, neuronal, and BC cells. In this work, we have investigated the KP across BC cell lines and tumour samples and observed highly divergent levels of several KP enzymes including indoleamine 2,3-dioxygenase (IDO1) and kynureninase (KYNU). In concurrent with metabolomics data, we identified high levels of KP metabolites, picolinic acid and kynurenic acid, in KYNU-high tumours. We investigated the effects of KP metabolites in BC cell lines and observed that, 3-hydroxyanthranilic acid (3-HAA) significantly decreases cell growth. Of the cell lines, 3-HAA had the greatest effect on cell growth in MCF-7 cells (p-value <0.001, $\log_2$ fold change of -4.8). To further investigate this effect, we treated three BC cell lines (with varying KYNU levels and 3-HAA effect on cell growth) with 3-HAA and performed proteomics analysis. The results of the proteomics and Gene Ontology (GO) enrichment analysis of significantly up-regulated proteins (p-value <0.05) in MCF-7 cells revealed molecular functions including leucine transporter, dehydrogenase, and monooxygenase activity. The mechanism behind these functions is not well-established but appears to involve AKR1C1, AKR1C3, SLC7A5, and SLC3A2. These proteins may reveal targetable vulnerabilities for high-KYNU and highly 3-HAA sensitive cell lines. The results of this research suggest a role for the kynurenine pathway in BC biology and understanding KP metabolite function and regulation in BC could offer essential information that may lead to the development of new targeted cancer therapies.

ACKNOWLEDGEMENTS

This research was conducted within the Biology Department at the University of Prince Edward Island.

Firstly, I would like to thank my supervisory committee: Dr. J Patrick Murphy and Dr. Joel Ross. Their meaningful feedback and support were invaluable to the conduction and communication of my research. I would like to further extend my thanks to my supervisor Dr. J Patrick Murphy for his encouragement and assistance. His mentorship was key to the completion of this project.

I would also like to acknowledge my colleagues in the Murphy Laboratory for their help with experimental procedures. I would like to thank Mukhayyo Sultonova, who taught me many technical skills that were invaluable to this project. I would also like to thank my fellow Murphy Lab members for providing me with a positive and encouraging work environment.

I would also like to thank the University of Prince Edward Island and members of the Biology Department. I am very grateful to have had the opportunity `to conduct this research.

Lastly, I would like to thank my friends and family for their support outside of the lab.

TABLE OF CONTENTS

LIST OF FIGURES

LIST OF ABBREVIATIONS

Acetonitrile (ACN)

Aldo-keto reductase (AKR)

Ammonium persulfate (APS)

Anthranilic acid (AA)

Bicinchoninic acid (BCA) assay

Bovine serum albumin (BSA)

Breast Cancer (BC)

Dimethyl sulfoxide (DMSO)

Dithiothreitol (DTT)

Dulbecco's modified eagle medium (DMEM)

Enhanced chemiluminescence (ECL)

Epidermal growth factor receptor 2 (HER2)

Estrogen receptor (ER)

Estrogen receptor 1 (ESR1)

Fetal Bovine Serum (FBS)

Formic acid (FA)

Gene Ontology (GO)

Hepatocellular carcinoma (HCC)

High performance liquid chromatography (HPLC)

Human aryl hydrocarbon receptor (AHR)

Hydroxyanthranilate 3,4-dioxygenase (HAAO)

Indoleamine 2,3-dioxygenase (IDO1)

Interferon-γ (IFN- γ)

Kynurenic acid (KA)

Kynurenine 3-monooxygenase (KMO)

Kynureninase (KYNU)

Kynurenine (Kyn)

Kynurenine aminotransferases (KATs)

Kynurenine Pathway (KP)

Lactate dehydrogenase (LDH)

Liquid chromatography with tandem mass spectrometry (LC MS/MS)

Nuclear factor κB (NF-κB)

Phosphate-buffered saline (PBS)

Progesterone receptor (PR)

Proteome integral solubility alteration (PISA)

Radio-Immunoprecipitation Assay (RIPA)

Reactive oxygen species (ROS)

Sodium dodecyl sulfate (SDS)

Sodium dodecyl sulphate-polyacrylamide gel electrophoresis (SDS-PAGE)

Tandem mass tag (TMT)

Tetramethylethylenediamine (TEMED)

Triple-negative BC (TNBC)

Tryptophan (Trp)

Tumour necrotic factor-α (TNF- α)

Quinolinic acid (QUIN)

2-amino-3-carboxymuconate-6-semialdehyde decarboxylase (ACMSD)

3-Hydroxyanthranilic acid (3-HAA)

3-Hydroxykynurenine (3-HK)

INTRODUCTION

Cancer is a leading cause of death worldwide and its incidence is on the rise (Sung et al., 2021). Female breast cancer (BC) is the most widely diagnosed cancer with an estimated 2.3 million new cases in 2020, accounting for 1 in 4 of all cancer cases (Sung et al., 2021). BC is among the top 5 causes of cancer mortality worldwide among women and the second leading cause of cancer related death in Canadian women.

Altered metabolism has long been observed in cancers to sustain their malignant characteristics (Vander Heiden et al., 2009). In BC, oncogenes, and other cancer-driver genes such as the estrogen receptor may enable metabolic changes resulting in differential enzyme expression (Mishra & Ambs, 2015). Therefore, cancer cells may have greater dependency on different enzymes and metabolites than normal cells (Mishra & Ambs, 2015). Emerging evidence indicates that specific metabolites, called oncometabolites, can support BC's malignant alterations, and promote carcinogenesis, signal transduction, and immune responses (Mishra & Ambs, 2015). Understanding oncometabolite function and regulation across BC subtypes can offer essential information to develop targeted BC therapies that selectively kill cancer cells depending on their unique characteristics.

Current research suggests the kynurenine pathway (KP) (Fig. 1) is implicated in immunosuppression and tumour growth, making it a possible therapeutic target (Heng et al., 2020). The KP plays a critical physiological role in the catabolism of tryptophan (Trp) to

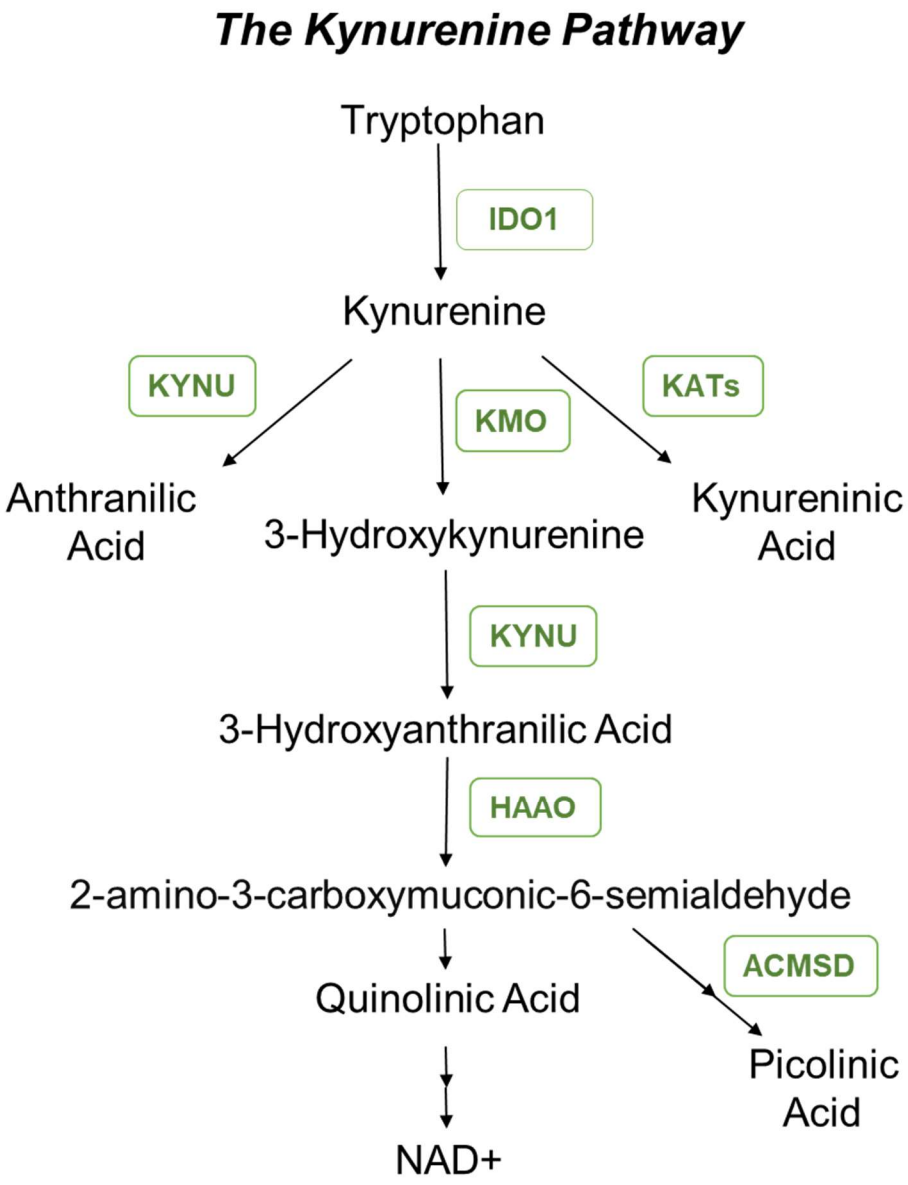

Figure 1. **Illustration of the kynurenine pathway, the catabolism of tryptophan to synthesize NAD+ for cellular energy.** The enzymes are shown in green. (IDO1 = indoleamine 2,3-dioxygenase, KMO = kynurenine 3-monooxygenase, KATs = kynurenine aminotransferases, KYNU = kynureninase, HAAO = hydroxyanthranilate 3,4-dioxygenase, ACMSD = 2-amino-3-carboxymuconate-6-semialdehyde decarboxylase)

produce nicotinamide adenine dinucleotide (NAD+) for cellular metabolism (Ghafouri-Fard et al., 2020). In addition, the KP contains several intermediates, which have been shown to have a bioactive role in immune, neuronal, and BC cells (Heng et al., 2016) with poorly understood mechanisms.

The goal of this research project was to investigate the effects of kynurenine pathway intermediates on BC cells. To accomplish this, we performed cell proliferation assays using cell counting on a subset of BC cell lines treated with KP metabolites. We also examined KP enzyme expression levels across these BC cell lines and tumour samples using western blotting. We examined tumour metabolomics data in combination with western blotting band intensities to identify metabolites present in high-KYNU tumours. Lastly, we performed proteomics on various BC cell lines after treatment with KP metabolites for complete proteome analysis.

LITERATURE REVIEW

Overview of Breast Cancer Incidence and Treatment

Of the 18.1 million cancer cases worldwide in 2020, BC was the most diagnosed with an estimated 2.3 million cases (11.7% of total cases) and these rates are on the rise (Sung et al., 2021). BC is now the leading cause of cancer death for women worldwide surpassing lung cancer and accounting for 15.5% of the 4.4 million cancer deaths for females in 2020 (Sung et al., 2021).

BC treatment is guided by the molecular properties of the tumour (Girithar et al., 2023). BC can typically be classified into subtypes depending on their expression of epidermal growth factor receptor 2 (HER2), estrogen receptor (ER), and progesterone receptor (PR). The four main subtypes include Luminal A (ER and PR positive), Luminal B (ER and HER2 positive), HER2-positive, and triple-negative BC (TNBC) which lack expression of all three receptors (Wang et al., 2021). The use of this classification is fundamental for guiding the administration of targeted therapies such as hormonal and HER-2-targeted therapy (Yeo & Guan, 2017). The luminal A subtype has the best prognosis followed by luminal B, HER2-enriched, and TNBC (Girithar et al., 2023; Cheang et al., 2009). Approximately two-thirds of BCs are ER and/or PR positive and can generally be treated using hormone therapy to minimize or block estrogen levels (Cheang et al., 2009). About 15% of BCs express HER-2, and these tumours can be treated using a monoclonal antibody targeting HER2 (trastuzumab), and/or adjuvant chemotherapy (Cheang et al., 2009). TNBCs typically have the lowest survival rates and are harder to treat because of the

reduced targeted therapies available due to the lack of HER2, ER, and PR. Other common BC treatment options include surgery, chemotherapy, and radiation therapy, which are highly invasive and nonspecific.

Despite the advancements in cancer treatment, cancer remains a leading cause of death worldwide and BC remains the leading cause of death for women, highlighting the need for more specific and effective treatments options. Of these cancer deaths, greater than 90% are caused by metastasis (Ganesh & Massagué, 2021). Further cancer research is warranted and necessary for improving metastatic cancer treatments.

Breast Cancer Metabolism

Cellular metabolism reprogramming has long been observed in cancer cells and has been recognized as a hallmark of cancer (Hanahan & Weinberg, 2011). Cancer cells alter their metabolism to support their malignant characteristics including invasive tumour growth, tissue remodeling, cancer metastasis, and uncontrolled cell proliferation (Mishra & Ambs, 2015). Given the nutrient and energy requirements of cancer cells, their metabolic requirements differ significantly from normal cells. Cancer cell metabolism can induce tumour vascularization and inflammation, inhibit immune response, and function as a protectant from cancer therapies (Mishra & Ambs, 2015). One well known metabolic shift observed in tumours is aerobic glycolysis, or the Warburg effect, characterized by the increased conversion of glucose to lactate in the presence of oxygen (Tu et al., 2022). The function of the Warburg effect is to increase the rate of glucose uptake to provide the tumour cells with glycolytic intermediates for anabolic reactions (Lunt & Vander Heiden, 2011).

This dysfunctional metabolism is regulated by oncogenes and tumor suppressor genes (Mishra & Ambs, 2015). The oncogene, estrogen receptor 1 (ESR1), encodes for estrogen receptor which is known to play a role in BC. ESR1 may enable metabolic changes explaining the large metabolite differences observed between ER-positive and ER-negative tumours (Mishra & Ambs, 2015). Two cancer related genes, MYC and TP53, have been found to be involved in altering BC metabolism (Mishra & Ambs, 2015). Through the process of metabolic shift, certain subsets of metabolites, termed oncometabolites, develop vital metabolic functions in cancer cells. These oncometabolites may support cell growth, protect the cancer cells, or have a role in signal transduction (Mishra & Ambs, 2015). The metabolic shifts observed in cancer cells provide them with proliferative advantages but are also potential targets for cancer therapies (Tu et al., 2022). Understanding BC metabolism amongst subtypes will provide opportunities for new metabolism-based targeted therapies.

Kynurenine Pathway

Tryptophan (Trp) is an essential amino acid required for protein synthesis, which must be obtained through diet. Trp has many important metabolic functions including being a precursor for many physiologically important metabolites (Badawy, 2017). Once ingested through diet, Trp has two metabolic fates. First, Trp may be distributed to cells and tissues through the bloodstream for use in protein synthesis, production of neurotransmitters serotonin and melatonin, and other functions (Colabroy & Begley, 2005). Second, Trp can be degraded by one of four degradation pathways (Moffett & Namboodiri, 2003). Of the four pathways, the kynurenine pathway (KP) is responsible for approximately 95% of tryptophan degradation

(Badawy, 2017). The KP plays a critical physiological role in the catabolism of tryptophan (Trp) to produce nicotinamide adenine dinucleotide (NAD+) for cellular metabolism (Ghafouri-Fard et al., 2020). The KP has also been identified to have a second biological role in regulating the immune system (Frumento et al., 2002). Given the pathway's involvement in regulating the immune system, the KP has been found to be elevated under inflammatory conditions such as cancers (Girithar et al., 2023). Current research suggests various links between the KP and tumour growth, making it a possible therapeutic target.

The most well studied enzyme in the KP, Indoleamine-2,3-dioxygenase (IDO1), catalyzes the first and rate-limiting step in the pathway by converting Trp to kynurenine (Kyn) (Hornyák et al., 2018). One mechanism of KP immunosuppression in cancers is the overactivation of IDO1 depleting Trp from the microenvironment. This depletion reduces Trp availability required for antitumor T cells and natural killer (NK) cells, ultimately hindering the immune system (Fallarino et al., 2002). IDO1 is transcriptionally upregulated by pro-inflammatory cytokines in the cancer microenvironment such as interferon-γ (IFN- γ) and tumour necrotic factor-α (TNF- α) and downregulated by anti-inflammatory cytokines such as interleukin (IL)-10 and IL-4 (Girithar et al., 2023). High levels of IDO1 lead to elevated levels of Kyn, which is a signalling molecule and ligand of human aryl hydrocarbon receptor (AHR) known to suppress cellular immune response and promote cancer development (Mishra & Ambs, 2015). Although IDO1 is expressed in some tumours, cancer therapies using IDO1 inhibitors have largely been unsuccessful (Hornyák et al., 2018).

Compared to IDO1, there is less known about the function of the other KP enzymes in BC. Kynurenine monooxygenase (KMO), downstream of IDO1, catalyzes the conversion of L-kynurenine to 3-hydroxykynurenine (3-HK) (Lu et al., 2020). KMO has been found to be

upregulated in TNBC and is most highly elevated in invasive BC compared to other cancers (Lai et al., 2021). KMO amplification has been associated with worse survival and malignant characteristics (Heng et al., 2020). Upregulation of KMO in hepatocellular carcinoma (HCC) has been found to cause alterations in the KP and promote cancer development (Lu et al., 2020). Therefore, the downregulation of KMO could inhibit cell proliferation and prevent cancer growth. Kyn and 3-HK (downstream of KMO) can also be converted into anthranilic acid (AA) and 3-hydroxyanthranilic acid (3-HAA) by kynureninase (KYNU), respectively. Of these two, 3-HAA has been identified as the main product, which is later converted to NAD+, while AA is produced when KYNU is fully saturated (Al-Mansoob et al., 2021). Further analysis of the Molecular Taxonomy of Breast Cancer International Consortium (METABRIC) dataset has also revealed elevated levels of KMO and KYNU expression in all three BC subtypes (luminal, TNBC, and HER2) compared to the healthy control (Heng et al., 2020). However, KYNU overexpression in mice inhibits BC cell proliferation and therefore may suppress tumour development (Lui et al., 2019). MTT assays of MCF7 and MDA-MB-231 cells transfected with KYNU expression plasmid revealed overexpression of KYNU, slowed proliferation, and fewer colonies (Lui et al., 2019). Another study proposed a link between KYNU and the nuclear factor κB (NF-κB) pathway, which is involved in tumour invasion and metastasis (Welz, 2019). The study suggests that KYNU expression may play a role in tumour cell invasion and may be correlated with TNF.

Increasing evidence shows that because of cancer's altered metabolism, several oncometabolites may promote tumorigenesis. KP metabolites 3-HK, 3-HAA, and quinolinic acid (QUIN) have also been shown to suppress anti-tumour T-cells (Girithar et al., 2023). Several KP enzymes and metabolites are known to be cytotoxic, including QUIN (which acts as an NMDA

receptor agonist), AA, 3-HAA, and 3-HK (Braidy et al., 2009). High levels of these metabolites have been associated with low levels of NAD+ and increased release of lactate dehydrogenase (LDH), which correlates with cell death and toxicity in neurons and astrocytes (Braidy et al., 2009). These metabolites may have anticancer effects favourable for increasing the efficacy of BC immunotherapies (Hornyak et al., 2018; Lu et al., 2020). Although several KP intermediates have been shown to have bioactive roles in immune and neuronal cells (Heng et al., 2020), their mechanisms of action and role in breast cancer biology are poorly defined. Present research has suggested the implication of the KP in breast cancer (Heng et al., 2020) but it is not fully understood. Defining the function and regulation of KP intermediates in breast cancer cells may reveal metabolic vulnerabilities for breast cancer.

MATERIALS AND METHODS

Cell lines, Metabolite Treatments, and Tissues

Human BC cell lines (MCF-7, HCC-1806, MDA-MB-468, MDA-MB-231, SKBR-3, BT474, MDA MB 453, and SUM149) were cultured in Dulbecco's Modified Eagle Medium (DMEM) (HyClone; SH30022.01) supplemented with 10% Fetal Bovine Serum (FBS) (Gibco; 2095193) and 1% Antibiotic-Antimycotic (VWR; CA45000-616). The cells were incubated at 37°C and 5% CO_2. To obtain cell lysates for western blotting, the eight cell lines in cell culture were each seeded in a 15 cm plate at 500,000 cells seeding density. Once the cells reached 90% confluency, they were harvested in Radio-Immunoprecipitation Assay (RIPA) lysis buffer (50mM TrisHCl, (pH 7.6), 100 mM NaCl, 0.1% sodium dodecyl sulfate (SDS), 1% Triton x100, 0.5% sodium deoxycholate, Milli-Q water, complete Mini protease inhibitor cocktail tablet), prechilled to 4°C. The cell lysates were stored at -80°C.

For the metabolite treatment experiment, the eight cell lines were each seeded in a 6 well plate at 10,000 cells per well. After 48 hours, each cell line was treated with 200 µM of a KP metabolite in a respective well using 0.5% dimethyl sulfoxide (DMSO) (Sigma-Aldrich; D8418) as a vehicle control. The KP metabolites include kynurenine (Sigma; K8625), anthranilic acid (Sigma; A89855), 3-hydroxykynurenine (3-Hydroxy-DL-kynurenine, Sigma-Aldrich; H1771) and 3-hydroxyanthranilic acid (97%, Sigma-Aldrich; 148776). Five days after the treatment, the media was aspirated, cells were washed with sterile 1X Phosphate-Buffered Saline (PBS) (Corning; 21-040-CV), and 150 µL of 0.25% trypsin (HyClone; SH40042.01) was added to each

well. The cells were incubated at 37°C until adherent cells detached from the plate. After incubation, 200 µL of media was added to each well. For each treatment group, 10 µL of cells was mixed with 10 µL of trypan blue stain and 10 µL of the mixture was transferred to each side of a counting slide. The number of live cells were counted for each side of the slide using the Countless 3 automated cell counter.

The lab of Carman Giacomantonio at Dalhousie University obtained TNBC tumour samples from Nova Scotia Health Authority. They lightly homogenized the fresh frozen samples using a razor blade and split the frozen tissue into equal portions. Half of the samples were resuspended in Proteome Integral Solubility Alteration (PISA) lysis buffer (1 mM MgCl2 and 0.5% NP-40 in 1X PBS, protease inhibitor cocktail). The lysates in PISA buffer were then shipped to the Murphy Lab at the University of Prince Edward Island for western blotting and were stored at -80°C. The other half of the samples were suspended in 80% ice cold methanol for untargeted liquid chromatography with tandem mass spectrometry (LC MS/MS) based metabolomics done at Dalhousie University.

For proteomic analysis, three cell lines, MDA-MB-468, MCF-7, and HCC-1806 were each plated into six 15 cm plates at 500,000 cells. After 48 hours, three of the plates for each cell line were treated with 200 µM of KP metabolite 3-HAA, while the remaining three plates were treated with a final concentration of 0.5% DMSO as a control (the HCC-1806 cell line was not treated with DMSO). Forty-eight hours after treatment, the media was aspirated off, the cells were washed twice with PBS and harvested for proteomics in a RIPA lysis buffer prechilled to 4°C. Cell lysates were stored in 1.5mL tubes at -80°C.

Protein Lysate Preparation

Cell lysates were thawed from -80°C and then kept on ice. Protein lysates were sonicated for 20 seconds with the sonifier set to continuous mode at 20 amplitude. This was repeated three times with a 1-minute rest on ice between cycles then lysates were spun in the centrifuge for 15 minutes at 20,000 x G. The supernatant containing all soluble proteins was transferred to new tubes and stored on ice.

BCA Assay

A Bicinchoninic acid (BCA) assay was used to quantify the total protein in the samples. A 10 mg/mL Bovine Serum Albumin (BSA) stock was made and diluted to 2 mg/mL in 1x PBS. This was serially diluted with 1x PBS to produce concentrations of 1000 µg/mL, 500 µg/mL, 250 µg/mL, 125 µg/mL, and 62.5 µg/mL. 1x PBS was used as a control (0 µg/mL). 20 µL of the standard concentrations were loaded onto a 96-well plate in duplicate. The lysate samples were diluted 1:5 with 80 µL of 1x PBS. 20 µL of the diluted lysates were loaded in duplicate into a BCA plate. The BCA reagent was prepared by combining enough reagent A and reagent B (ThermoFisher; 23225) in a 50:1 ratio to add 220 µL of the BCA reagent into the wells containing the samples. The plate was incubated at 37°C for 30 minutes and then read using an absorbance spectrophotometer at 595nm absorbance. Total protein concentrations of the lysates were calculated using Excel.

Sodium Dodecyl Sulphate-Polyacrylamide Gel Electrophoresis (SDS-PAGE)

A 12% resolving gel was made by combining 4.5 mL 40% acrylamide, 3.75 mL 1.5M Tris-HCL, 150 µL 10% SDS, 6.53mL Milli-Q water, 75 µL 10% ammonium persulfate (APS), and 7.5 µL tetramethylethylenediamine (TEMED). The 12% resolving gel was poured into the electrophoresis tray and solidified for about 45 minutes. Approximately 100 µL of isopropyl alcohol was added on top of the gel to help remove bubbles and keep the gel from drying out.

A 4% stacking gel was made by combining 1.5 mL 40% acrylamide, 3.78 mL 0.5M Tris-HCL, 150 µL 10% SDS, 9.48 mL Milli-Q water, 75 µL 10% APS, and 15 µL TEMED. Once the resolving gel had solidified, the stacking gel was poured on top and a 1.5 cm well comb was inserted into the top of the tray. The gel was let to solidify for 30 minutes and then was stored at 4°C.

Western Blotting

The cell lysates from the eight human BC cell lines and tumour samples were used for western blotting. The lysates from the cell lines were diluted in RIPA buffer to make 20 µL of sample with 20 µg of protein according to the protein concentrations from BCA assay. This was also done for the tumour samples lysates, but they were diluted in PISA buffer instead of RIPA. Lysates were diluted with 6X loading buffer containing 1M Tris-HCL, 4% SDS, 5% Dithiothreitol (DTT), 20% glycerol, 0.004% bromophenol blue. Then, the lysates were heated up on a hot plate at 95°C for 5-10 minutes and centrifuged for 10 seconds. 20 µL of each protein sample was loaded into each well and the gel was run at 110V for about 1.5 hours using

Tris/Glycine/SDS buffer (25mM Tris, 192 mM glycine, and 0.1% SDS). This was followed by transfer onto a nitrocellulose membrane using transfer buffer (192 mM glycine, 25 mM Tris in 20%(v/v) methanol), kept on ice and ran for an hour at 110V.

The membrane was blocked with a using a solution of 1x PBST (1x PBS & 0.05% Tween) with 5% milk for an hour at 150 rpm. Antibodies were diluted at 1:1000 µg/mL ratio of primary antibody in solution (1x PBST with 5% milk) and added to the membrane overnight shaking at 125 rpm. The next day, the membrane was rinsed three times with 1x PBST and 1:4000 diluted secondary antibody was added and incubated for an hour at 125 rpm. After an hour, the membrane was rinsed three times. The membrane was imaged using enhanced chemiluminescence (ECL) substrate (Fisher; PIA34075). The membrane was rinsed with 1x PBST and then stripped of antibodies using a mild stripping buffer (0.2 M glycine, 0.1% SDS, and 1% Tween) twice for 7 minutes at 200 rpm. The membrane was rinsed twice for 10 minutes in 1x PBST, blocked as previously described, and the steps were repeated for the next antibodies.

Proteomics

Reduce/Alkylate

The lysates from the three cell lines, MDA-MB-468, MCF-7, and HCC-1806 (3-HAA treatment and DMSO control), were reduced and alkylated for proteomic analysis. To reduce the disulfide bonds of the proteins, 1 µL of 0.5 M DTT was added to 100 µL lysate in PCR tubes and incubated at room temperature for 30 minutes. 2-Idodoacetamide (C_2H_4INO) was used as an alkylating agent to prevent reformation of disulphide bonds. 12 mM Iodoacetamide (IAA)

(Fisher; BP1408-1) was added to the samples and incubated in the dark at room temperature for 30 minutes.

SP3/Digest

Enough magnetic Sera-Mag SpeedBeads was prepared, in a 10:1 bead (50 µg/ml) to protein (25 µg) ratio, to add 5 µL of bead stock to each sample. The beads were put on magnets and the supernatant was removed, then the beads were rinsed twice with 200 µL of milli-Q water. The beads were resuspended in 50 µL of milli-Q water, aliquoted into new PCR tubes (5 µL per tube), and 25 µg of protein from the sample was added to the beads. 100% Ethyl alcohol was added to each sample to make a 50% ethanol mixture. Then, the samples were agitated for 10 minutes and placed on a magnet to remove the supernatant. The beads were rinsed with 200 µL of 80% Ethyl alcohol three times, 10 µL of 0.25 ng/µL trypsin was added, and they were incubated overnight at 37°C. The next day, the second digest was performed by adding 1 µL of 25 µg/µL of trypsin and the samples were incubated at 37°C for 2 hours. The supernatant was collected into a new tube, then the beads were rinsed with 5 µL of 200mM EPPS (except for 1806 samples) and the supernatant was collected.

TMT-Labelling

Following digest, 7.5 µL of MS-grade acetonitrile (ACN) (Fisher; A21 4) was added to the peptide samples to make the final concentration of ACN up to 30%. The samples were transferred to labelling tubes containing 5 µL of 18-plex Tandem Mass Tag (TMT) reagents (126, 127N, 127C, 128N, 128C, 129N, 129C, 130N, 130C, 131N, 131C, 132N, 132C, 133N, 133C, 132N, 134C, 135) and incubated for an hour at room temperature. Next, each sample was quenched with 5 µL of 5% hydroxylamine (Sigma; 159417) (prepared from powder) and

incubated for 10 minutes. Once the peptides were labelled, all the samples were combined into a single tube and 500 µL of 1% MS-grade formic acid (FA) (Fisher; A11750) was added.

Sep-Pak

The samples were desalted using a 100 mg tC18 Sep-Pak cartridge (Waters; WAT036820) in a vacuum manifold over a waste tube. The following solutions were loaded in order into the cartridge and let flow through at 1 drop per 5s: Methanol (500 µL), 1 mL of 50% ACN/1% FA, 1 mL of 1% FA (2x), labelled sample, 1 mL of 1% FA (2x). The cartridge was not run completely dry to ensure the resin was kept wet for the procedure. Next, the waste tube under the cartridge was discarded and replaced with a 1.5 mL Eppendorf tube for collection. The peptides were eluted by loading the following solutions in order into the cartilage and let run dry: 1mL of 50% ACN/1% FA and 500uL of 70% ACN/1% FA. The Eppendorf tube was removed from the vacuum and the peptides were dried overnight in a vacuum concentrator. The Sep-Pak column was discarded, and the vacuum chamber was rinsed with 1% FA.

HPLC

Dried peptides were resuspended in 90 µL of 5% ACN, 10 mM ammonium bicarbonate and sonicated twice for 12 s with sonifier set to continuous mode at 20 amplitude, resting for 1-minute on ice between cycles. The peptides were centrifuged at 20,000 x G for 5 minutes and the supernatant was transferred into a high-performance liquid chromatography (HPLC) vial. The peptides were subjected to HPLC using an Agilent 300Extend, 2.1 x 100 mm, 3.5-µM C18 column starting with 5% ACN, 10 mM ammonium bicarbonate. The peptides were eluted at flow rate of 250 µL/min using an elution gradient of 5% to 40% of 90% ACN, 10 mM ammonium bicarbonate. A total of 96 fractions were collected and combined into 12 total fractions by

combining every second fraction in each column of a 96-well rack alternating between odd and even fractions. For the first column, all the odd numbered fractions were combined, for the second column all the even numbered fractions were combined, and so on. The fractions were dried overnight in a vacuum concentrator.

Stage Tip

Dried peptide fractions were resuspended in 100 µL of 1% FA. Stage tips were prepared and placed into the centrifuge. The following solutions were loaded into each stage tip in order and spun for 3 minutes at 650 x G while keeping the resin wet: 50 µL Methanol, 100 µL 50% ACN/1% FA, 100 µL of 1% FA (2x, empty waste tube), 12 fractions, 100 µL of 1% FA (2x) (empty waste tube and add glass conical insert into stage tip apparatus), 50 µL of 50% ACN/1% FA, 30 µL of 70% ACN/1% FA and allow resin to dry. The glass conical was removed and placed into a new 1.5 mL Eppendorf tube. The fractions were dried in the vacuum concentrator for 1.5 hours. The samples were shipped to Harvard for mass spectrometry and samples were analyzed using an Orbitrap Fusion Lumos mass spectrometer (Thermo-Fisher Scientific, San Jose, CA) coupled with a Proxeon EASY-nLC 1200LC pump (Thermo-Fisher Scientific, San Jose, CA) using a FAIMS-HRMS2 method from Li et al. (2020).

Data Analysis

The LC-MS/MS data was analyzed using MSFragger (version 3.4) in FragPipe software (version 17.0) and searched against a protein sequence database on UniProt. Fixed modification on lysine and N-termini of peptides were set to 304.2071 Da and were set to 57.0215 Da on

cysteines. Variable modification on methionine was set at 15.9949 Da. The precursor mass tolerance was set to ±10 ppm and fragment mass tolerance to 0.02 Da for high-resolution data. Data were corrected for differences in protein abundance by multiplying by a correction factor. Analysis and visualization were done using R Studio where t-test p-values were calculated using genefilter package and adjusted using the Benjamini-Hochberg (B-H) algorithm. Statistical significance was defined as p-values <0.05. The B-H adjusted p-values revealed no significant differences, so non-adjusted p-values were used. Band intensities for the western blot of tumour samples were quantified using ImageLab software.

RESULTS

Kynurenine Pathway in Breast Cancer

There is strong evidence that the KP is associated with BC and several KP enzymes have been identified as potential targets for metabolism-based BC therapies (Girithar et al., 2023). Although the KP has shown a strong association with BC, the mechanism of action is poorly understood. To investigate this pathway, we assessed KP involvement in several BC tumour samples using western blotting and metabolomics (**Fig. 2A**). Western blot analysis of the tumour samples revealed highly divergent protein levels of KYNU and IDO1 (**Fig. 2B**). Using ImageLab, band intensities were quantified and three tumour samples, B380T, B390T, and B92T, were classified as KYNU-high tumours (**Fig. 2C**) while remaining tumour samples were classified as low-KYNU tumours. Metabolite abundance across tumour samples was determined by metabolomics using LC MS/MS. The metabolomics data was matched up with the western blot data and metabolite abundance was plotted against the ratio of high-KYNU to low-KYNU tumours (**Fig. 2C**). Analysis of this data revealed that several metabolites were highly abundant in the high-KYNU tumours compared to the low-KYNU tumours. Interestingly, two KP metabolites, kynurenic acid and picolinic acid, were highly abundant in the high-KYNU tumours as well as several other metabolites including Isobutyric acid, and Xanthine. These data suggest a role for the kynurenine pathway in BC tumours. To further investigate this pathway in BC, western blot analysis was performed on eight BC cell lines (MDA-MB-453, MDA-MB-468, BT474, SKBR-3, HCC-1806, MCF-7, SUM149, and MDA-MB-231) grown in cell culture (**Fig. 3A**). Much like tumours, the western blot analysis of the eight cell lines revealed highly

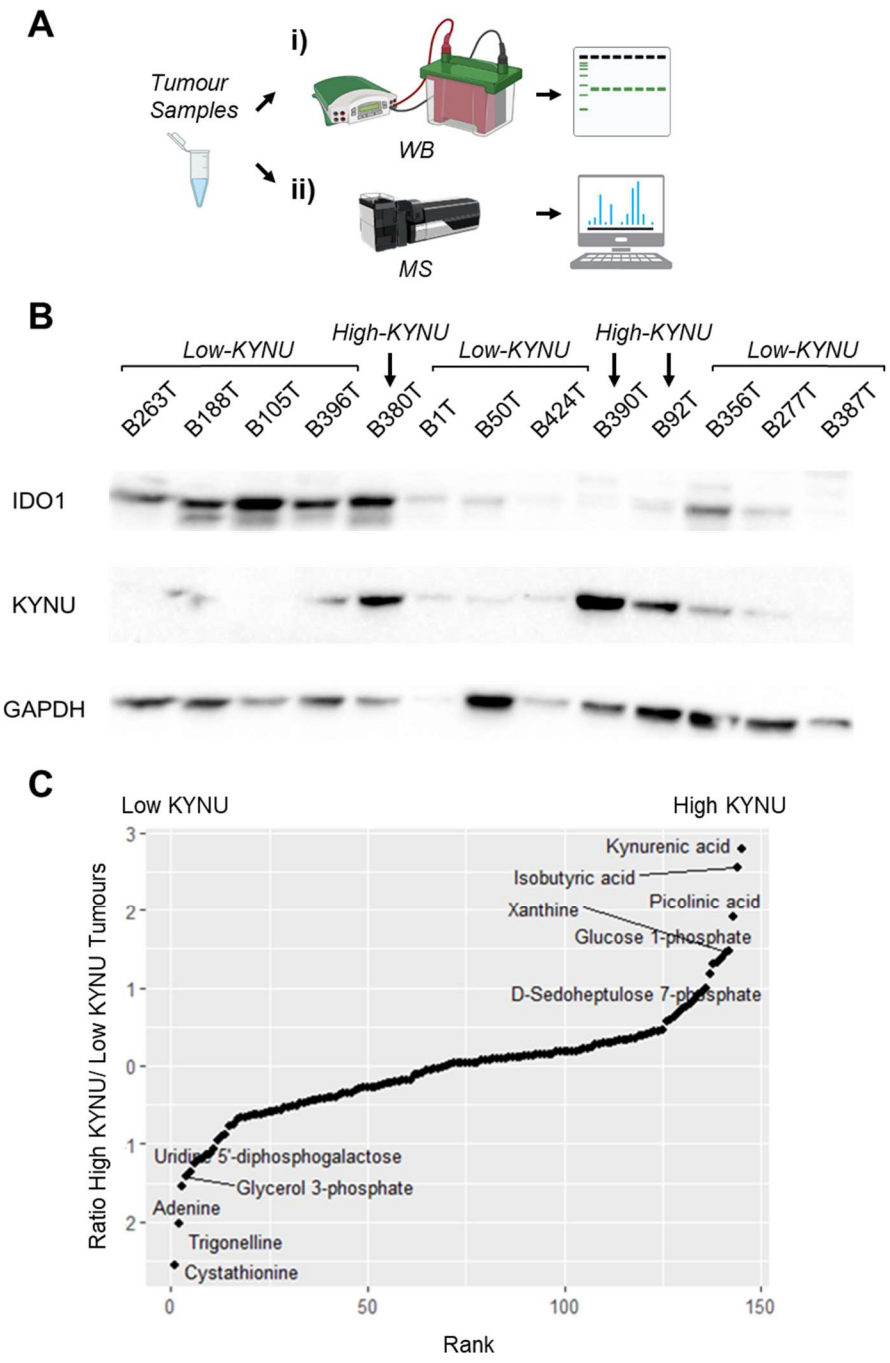

Figure 2. **Kynurenine pathway enzyme and metabolite abundance across breast cancer (BC) tumour samples. A)** Workflow for (**i**) western blotting (WB) and (**ii**) metabolomics on triple negative BC tumour samples from Nova Scotia Health Authority (MS= Mass Spectrometry) **B)** Western blot analysis of KP enzymes, IDO1, KYNU, and control GAPDH across a subset of BC tumours. Several KP enzymes were shown to be upregulated in some BC tumours. (KYNU-high tumours = B380T, B390T, B92T) **C)** Metabolite abundance across ratio of high-KYNU to low-KYNU tumours characterized by band intensities. Several metabolites, Kynurenic acid, Isobutyric acid, and Picolinic acid are highly abundant in the High-KYNU tumours compared to low-KYNU tumours.

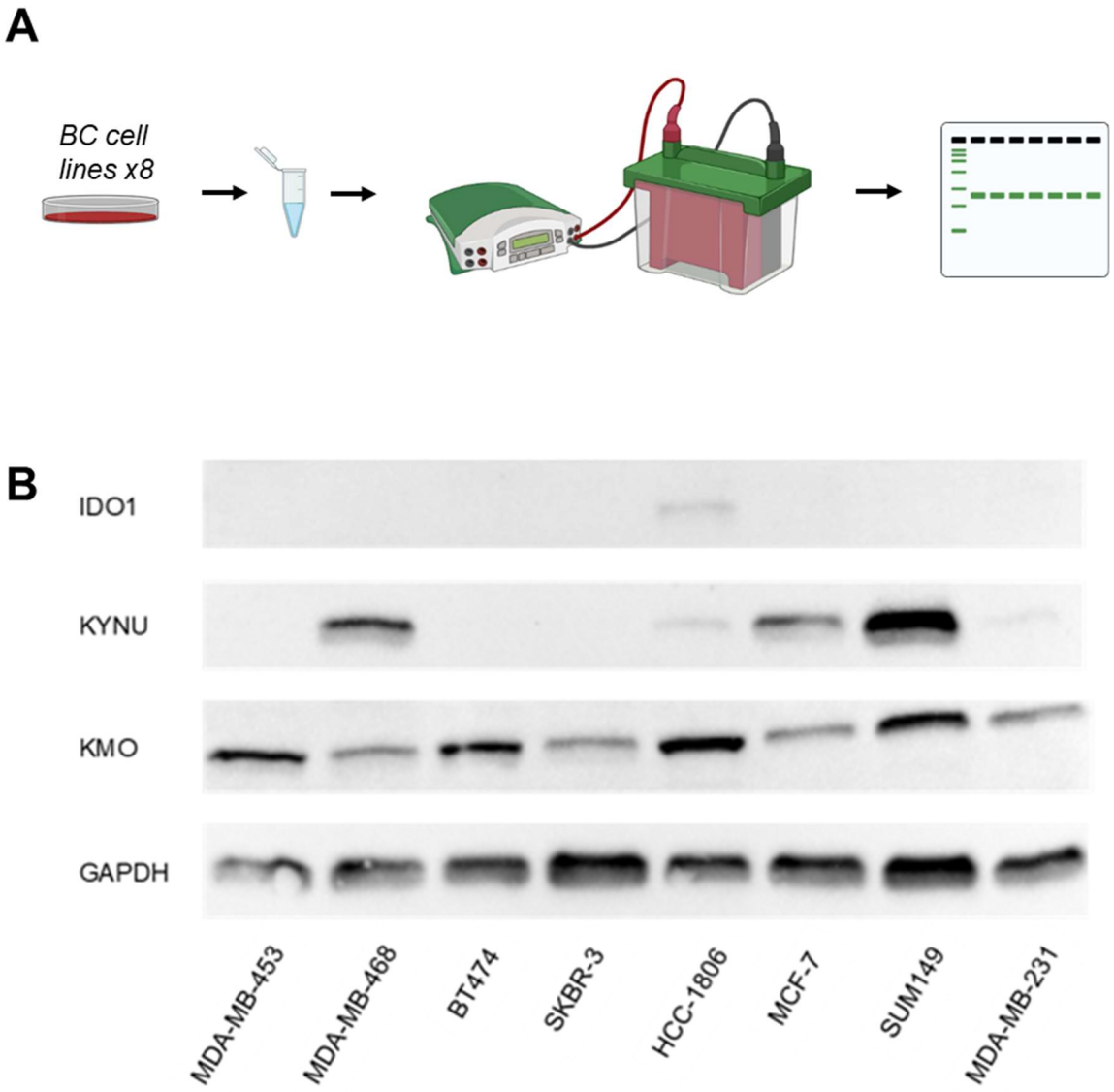

Figure 3. **Kynurenine pathway protein abundance across breast cancer (BC) cell lines. A)** Overview of experimental layout assessing the expression of several KP enzymes, IDO1, KYNU, KMO, and GAPDH (control) across a subset of eight human BC cell lines (MDA-MB-453, MDA-MB-468, BT474, SKBR-3, HCC-1806, MCF-7, SUM149, MDA-MB-231). **B)** Western blot analysis of KP enzymes across the subset of human BC cell lines. The first enzyme in the KP, IDO1, was minimally expressed across the eight cell lines. However, several KP enzymes downstream of IDO1 were shown to be upregulated in some BC cell lines. (GAPDH = Glyceraldehyde 3-phosphate dehydrogenase).

divergent protein levels of KYNU (**Fig. 3B**). However, the western blot revealed minimal IDO1 expression and relatively consistent KMO expression across cell lines. Three cell lines, MCF-7, MDA-MB-468, and SUM-149 had high KYNU expression, whereas the HCC-1806 cell line had low KYNU expression, and the remaining cell lines had minimal KYNU expression. Taken together, these data suggest that KYNU levels are highly differentially expressed across tumors and correlate with the production of known KP metabolites.

Effect of Kynurenine Metabolites

To determine the function and effect of KP metabolites in BC metabolism, eight BC cell lines were treated with four KP metabolites (AA, Kyn, 3-HK, 3-HAA) using 0.5% DMSO as a control (**Fig. 4A**). Five days after treatment, cell counting assays were performed to assess the effects of the metabolites. Analysis of the data revealed that 3-HAA decreased cell growth in all eight cell lines tested (**Fig. 4B**). Among the eight cell lines, there was a statistically significant decrease in cell growth in six of the cell lines (MCF-7, HCC-1806, SKBR3, MDA-MB-468, SUM149, MDA-MB-453) (p-value<0.05), with the greatest effect on cell growth seen in the MCF-7 cell line with a $\log_2$ fold change (treatment/control) of -4.8 (**Fig. 4C**). The 3-HAA treatment had the least effect on cell growth in the HCC-1806 cell with a $\log_2$ fold change (treatment/control) of -0.65.

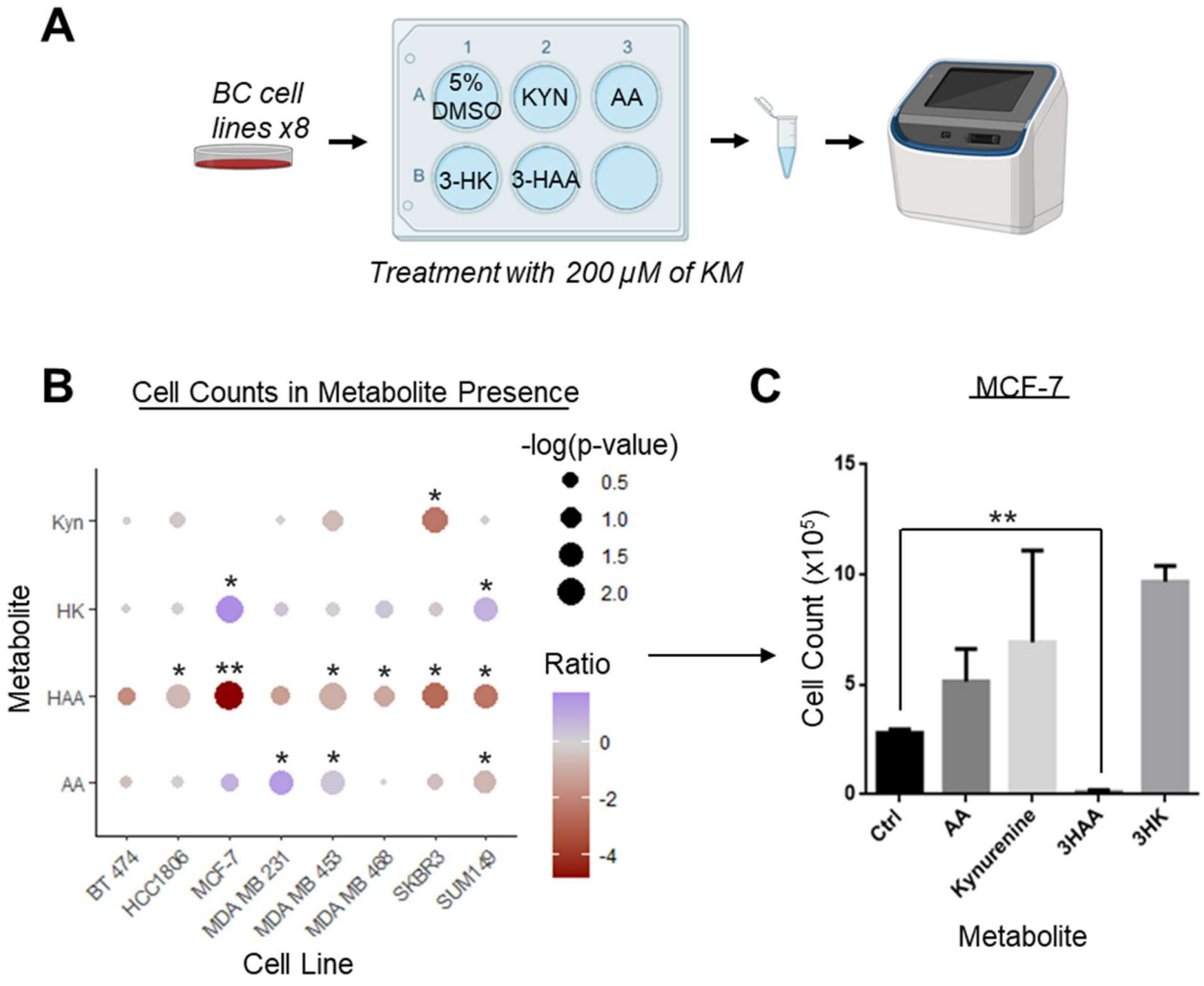

Figure 4. **Kynurenine metabolites effect on breast cancer (BC) cell growth. A)** Overview of the methodology for investigating the effect of kynurenine metabolites on cancer cells. Eight human BC cell lines were each seeded in six well plates at 10,000 cells per well. After 48 hours, each cell line was treated with 200 µM of a KP metabolite in a respective well. Cells were counted five days after treatment using a cell counter (n = 2). **B)** Analysis of relative cell count compared to control (0.5% DMSO) for each metabolite among the eight cell lines. Treatment decreased cell growth significantly in 6 of the 8 cell lines (t-test, p-value <0.05). Ratio represents the $\log_2$ fold change (treatment/control). (t-test, * = p-value <0.05, ** = p-value <0.01) **C)** Cell count for MCF-7 cell line across the four metabolite treatments. 3-HAA has the most significant effect on MCF-7 cell growth (t-test, ** = p-value <0.01). Error bars represent standard error of the mean (SEM). (KM= kynurenine metabolite, DMSO = dimethyl sulfoxide, AA = anthranilic acid, Kyn = kynurenine, 3-HK = 3-hydroxykynurenine, 3-HAA = 3-hydroxyanthranilic acid)

To further understand this effect, three BC cell lines (MCF-7, MDA-MB-468, and HCC-1806), with varying levels of KYNU expression and effect of 3-HAA on cell growth, were treated with 3-HAA (**Fig. 5A**). After 48 hours, the cells were harvested in the RIPA buffer for proteomics (**Fig. 5B**). To enable the detection of protein differences between treatments, we used an 18-plex TMT-based sample multiplexing, quantified the proteins using LC-MS/MS, and analyzed the data (**Fig. 5B-D**). Analysis of the data revealed many significant protein differences in all three cell lines between the control and treatment group (p-value<0.05). We identified 304 proteins that were significantly differentially expressed between the treatment and control group in the HCC-1806 cell line (p-value<0.05) (**Fig. 6A**). The top six proteins based on p-value, include DHRS7B, FBXO6, GOLPH3L, IL1B, LPCAT3, and STC1 (**Fig. 6B**). Of these proteins, IL1B was found to be the most significantly elevated in the treatment group with a $\log_2$ fold change of 1.93. Interestingly, STC1 was not expressed in the control group but was highly elevated in the treatment group. In the MCF-7 cell line, we quantified 498 significant protein differences between the treatment and control group (p-value<0.05) (**Fig. 7A**). The top six significantly differentially expressed proteins based on p-value (AARS1, AKR1C1, AKR1C3, FDFT1, INVS, and RB1) were plotted visually (**Fig. 7B**). AARS1, RB1, and FDFT1 were found to be downregulated in the treatment group compared to the control with $\log_2$ fold changes (treatment/control) of -0.39, -0.08, and -0.21, respectively. AKR1C1 and AKR1C3 were significantly upregulated in the treatment group with $\log_2$ fold changes (treatment/control) of 0.99 and 0.67, respectively. INVS was not expressed in the control group but was significantly elevated in the treatment group. In the MDA-MB-468 cell line, 833 proteins had significantly different expression in the treatment group compared to the control cells (p-value<0.5) (**Fig. 8A**). Among the top six significant proteins (based on p-value), CYP1B1 was the only protein that

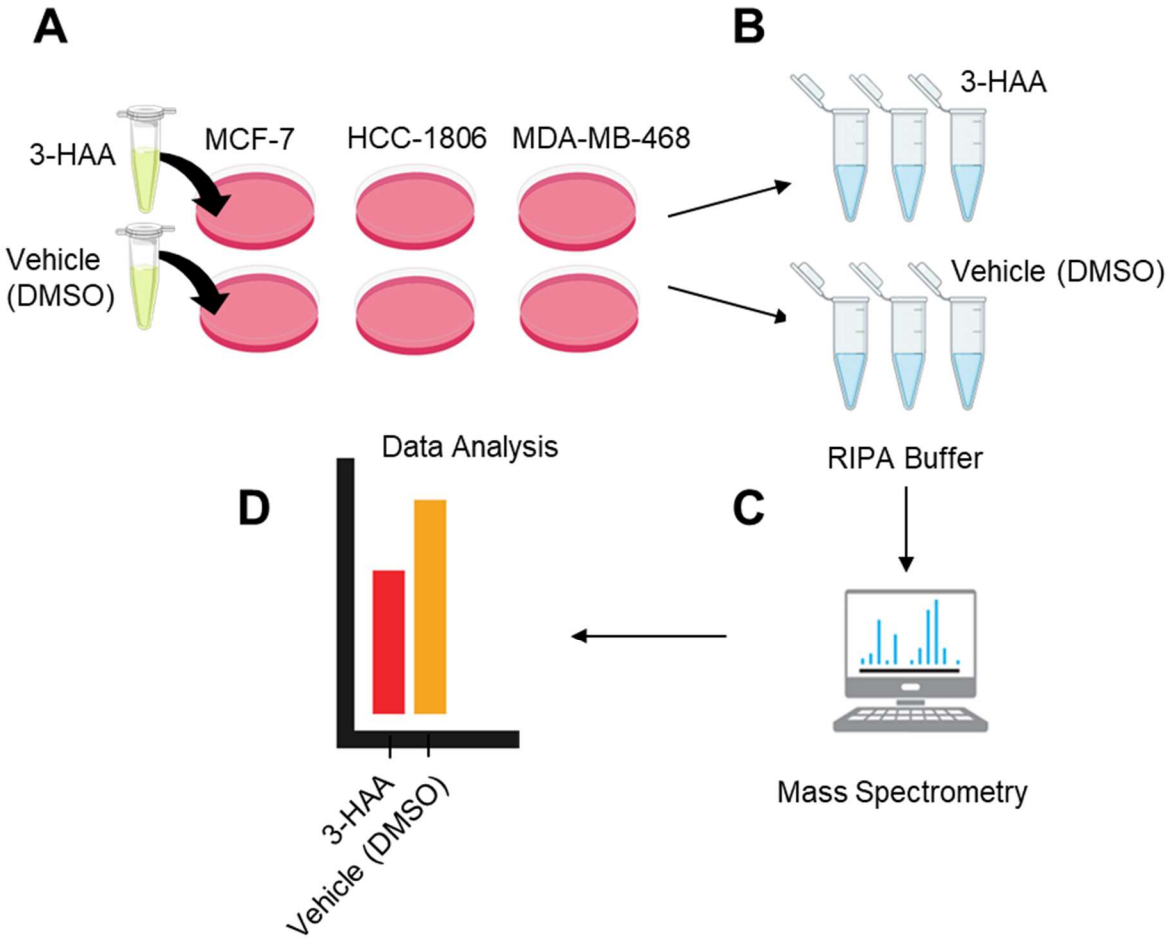

Figure 5. **Overview of proteomics workflow. A)** Three cell lines with varying KYNU expression and 3-HAA effect on cell growth (KYNU-High MCF-7 and MDA-MB-468 and KYNU-low HCC-1806) were treated with 200 µM of 3-hydroxyanthranilic acid (3-HAA) using 0.5% DMSO as a vehicle control (n =3). **B)** After 48 hours, the cells were harvested in RIPA buffer. **C)** The lysates were prepped for mass spectrometry and data was subjected to computational analysis. (KYNU = kynureninase, DMSO = dimethyl sulfoxide, RIPA = Radio-Immunoprecipitation Assay)

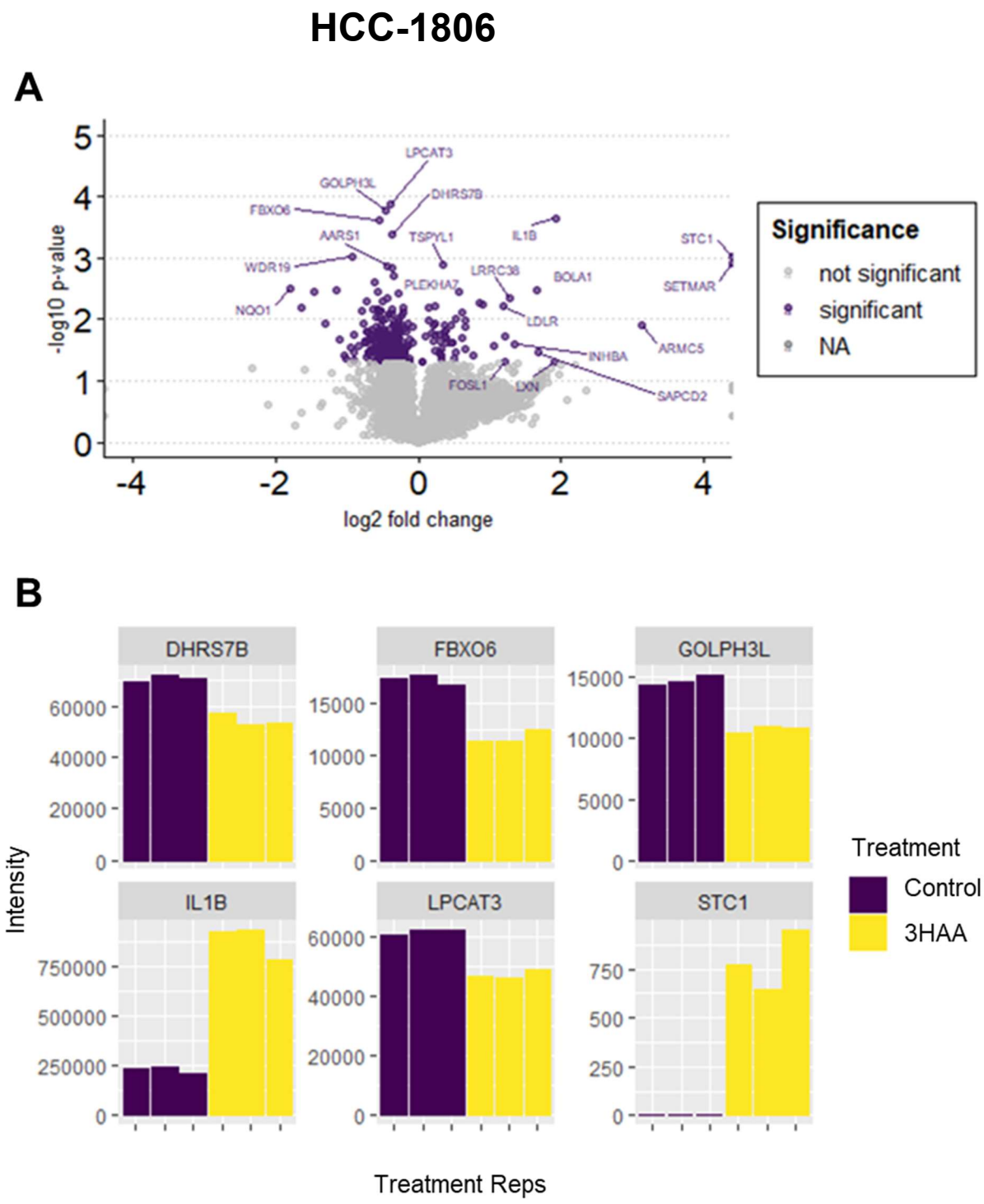

Figure 6. **Proteomic analysis of HCC-1806 cell line treated with 3-hydroxyanthranilic acid (3-HAA). A)** Volcano plot depicting differentially expressed proteins in HCC-1806 breast cancer (BC) cell line. Log_2 fold change of ± 4 plotted against the $-log_{10}$ of the p-value. BC cells treated with 3-HAA resulted in 304 significantly differentially expressed proteins compared to the control cells (n = 3, t-test, p-value <0.05). **B)** Barplot depicting the top six protein with most significant difference based on p-value (n = 3, t-test, p-value <0.05).

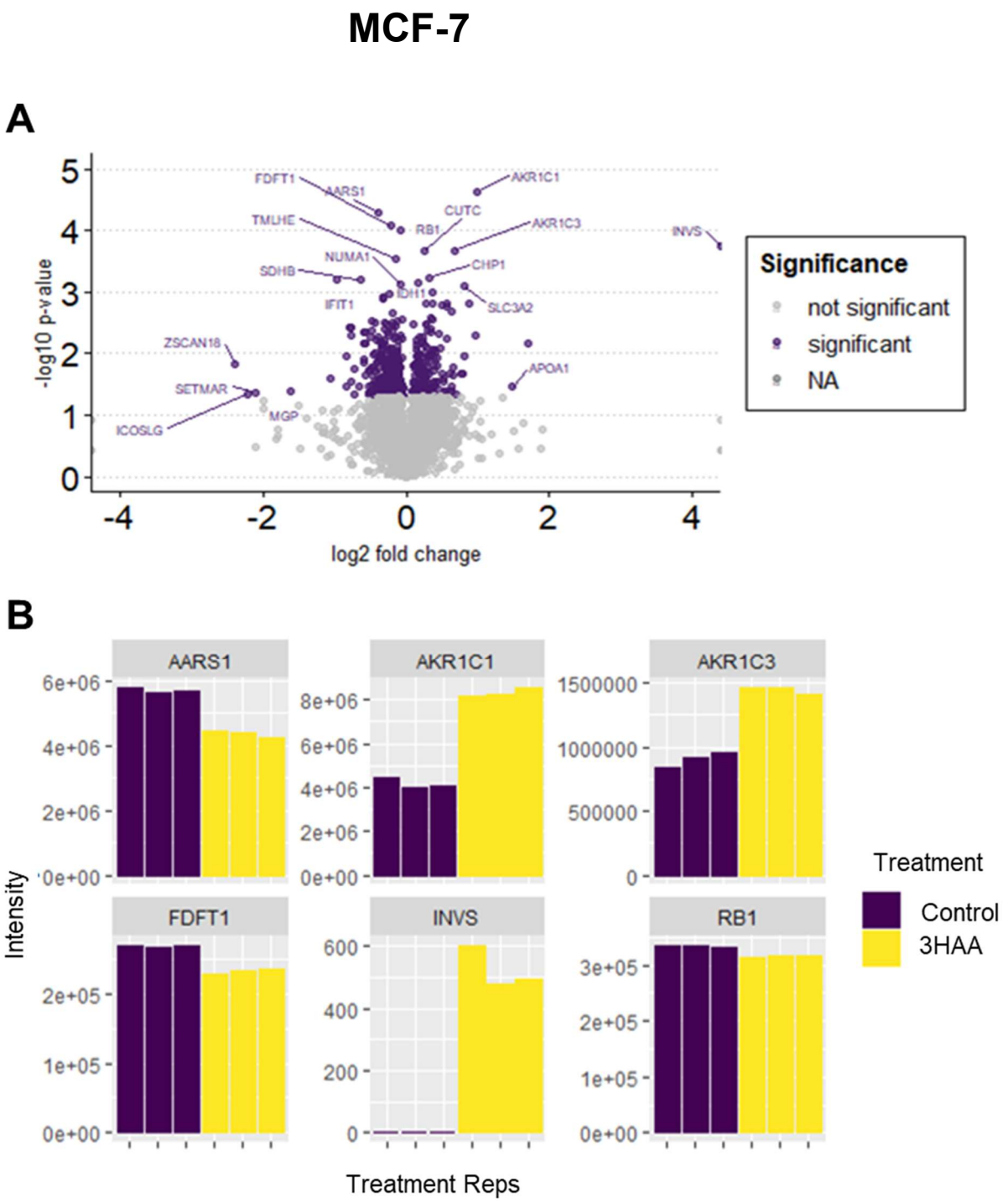

Figure 7. **Proteomic analysis of MCF-7 cell line treated with 3-hydroxyanthranilic acid (3-HAA). A)** Volcano plot depicting differentially expressed protein in MCF-7 breast cancer (BC) cell line. Log_2 fold change of ± 4 plotted against the $-log_{10}$ of the p-value. BC cells treated with 3-HAA resulted in 498 significantly differentially expressed proteins compared to the control cells (n = 3, t-test, p-value <0.05). **B)** Barplot depicting the top six proteins with most significant shift based on p-value (n = 3, t-test, p-value <0.05).

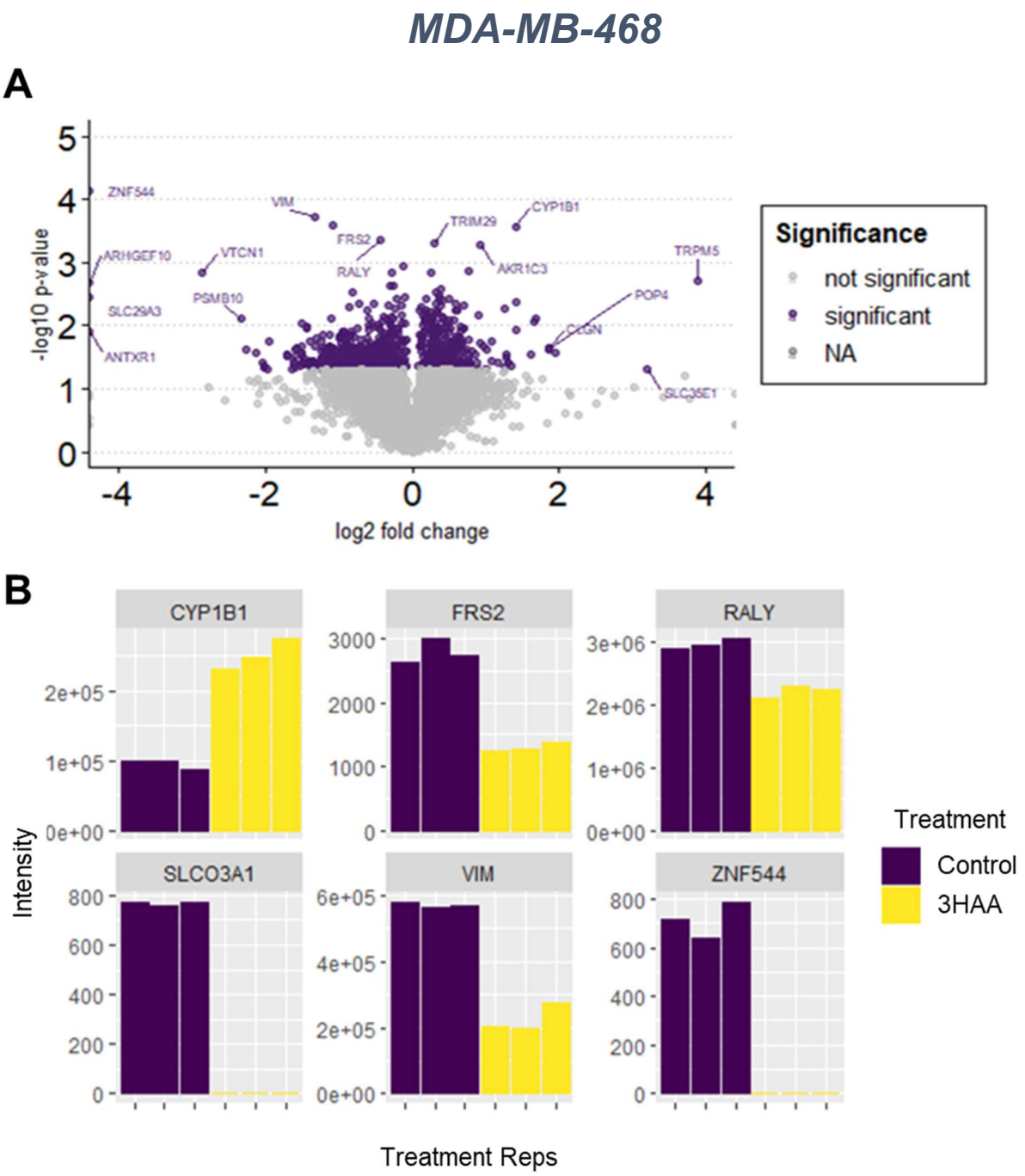

Figure 8. **Proteomic analysis of MDA-MB-468 cell line treated with 3-hydroxyanthranilic acid (3-HAA). A)** Volcano plot depicting protein shift in MDA-MB-468 breast cancer (BC) cell line. Log_2 fold change of ± 4 plotted against the $-log_{10}$ of the p-value. BC cells treated with 3-HAA resulted in 833 significantly differentially expressed proteins compared to the control cells (n = 3, t-test, p-value <0.05). **B)** Barplot depicting the top six protein with most significant shift based on p-value (n = 3, t-test, p-value <0.05).

was upregulated in the treatment group with a $\log_2$ fold change (treatment/control) of 1.4 (**Fig. 8B**). FRS2, RALY, VIM, were downregulated in the treatment group with $\log_2$ fold changes (treatment/control) of -1.09, -0.43, -1.34, respectively. SLCO3A1 and ZNF544 were expressed in the control groups but showed no expression in the treatment group.

Enrichment analysis on gene sets inspecting the molecular function of significantly different proteins revealed several over-represented molecular function Gene Ontology (GO) terms in the MCF-7 and MDA-MB-468 cell lines (FDR < 0.05) (p-values <0.05 and $\log_2$ fold change < -0.5 or > 0.5). (**Fig. 9A-C**). Among the significantly up-regulated proteins in MCF-7 cells, the GO term analysis revealed functions such as leucine transporter activity, dehydrogenase activity, and monooxygenase activity (**Fig. 9A**). Leucine transporter activity includes proteins in the solute carrier family (SLC) such as solute carrier family 3 member 2 (SLC3A2) (**Fig. 10A**). SLC3A2 was not significantly different among the two other cell lines, and thus, it may be related to 3-HAA's effect on MCF-7 cell growth. The molecular functions dehydrogenase activity, and monooxygenase activity include Aldo-keto reductase (AKR) proteins such as AKR1C1 and AKR1C3 (**Fig. 10B and 10C**). AKR1C1 and AKR1C3 were also significantly different in the HCC-1806 and MDA-MB-468 cell line, respectively (p-value <0.05, p-value <0.001). No statistically significant results were found from GO term analysis for significantly down-regulated proteins in MCF-7 cells. GO term analysis of significantly up- and down-regulated protein abundance in MDA-MB-468 cells revealed functions such as protein binding, RNA binding, and copper chaperone activity (**Fig. 9B and 9C**). Both MDA-MB-468 significantly up- and down-regulated proteins revealed molecular binding functions including the protein PHAX (**Fig. 11A**) and APOA1 (**Fig. 11B**), respectively. Unfortunately, enrichment analysis of significant proteins in the HCC-1806 cell line showed no statistically significant results (p-values <0.05 and $\log_2$ fold change < -0.5 or > 0.5).

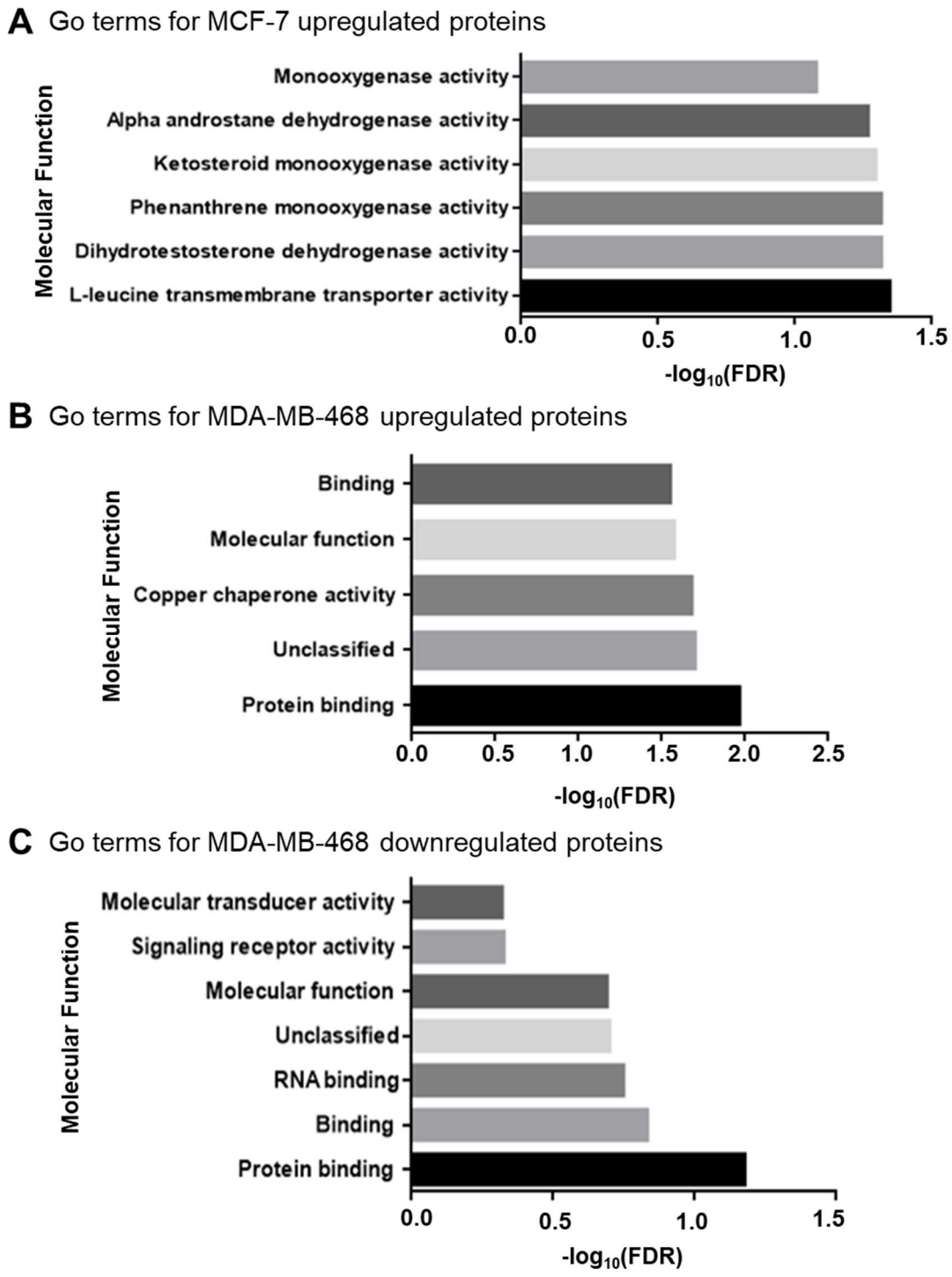

Figure 9. **Go terms for significantly differentially expressed proteins. A**) Go terms for significantly up-regulated proteins in MCF-7 cell line (n=3, t-test, $p<0.05$ and $\log_2$ fold change >0.5) **B**) Go terms for significantly up-regulated proteins and **C**) down-regulated proteins in MDA-MB-468 cell line (n=3, t-test, $p<0.05$ and $\log_2$ fold change >0.5 or <-0.5, respectively).

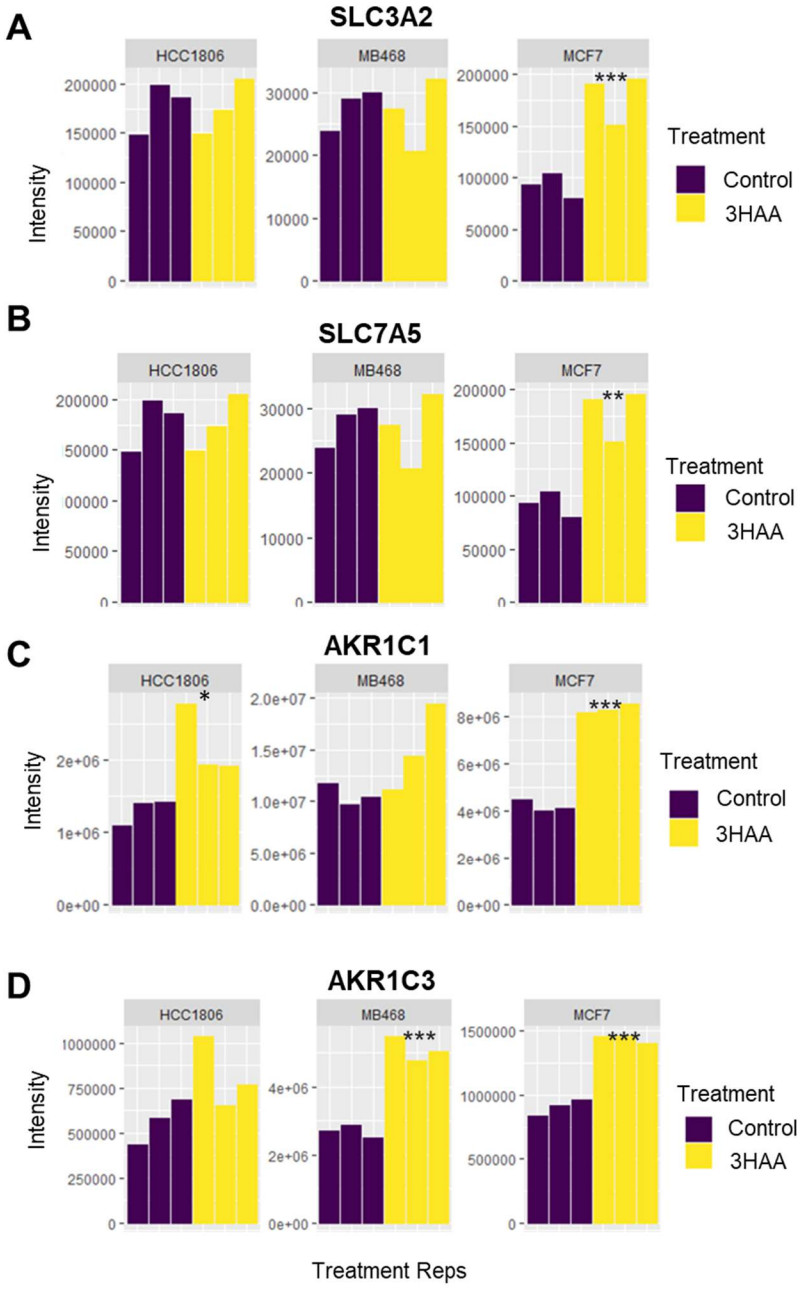

Figure 10. **Proteins matching the molecular function GO terms for significantly up-regulated proteins in MCF-7 cell line across all three cell lines. A-B)** Proteins SLC3A2 and SLC7A5, matching the leucine transporter activity GO terms, are significantly up-regulated in the MCF-7 cell line (n = 3, t-test; p-value <0.001, p-value <0.01, respectively). **C-D**) Aldo-keto reductase proteins matching the dehydrogenase and monooxygenase activity GO terms. AKR1C1 and AKR1C3 are significantly different in MCF-7 cell line (p-value <0.001), and HCC1806 (p-value <0.05) and MDA-MB-1806 (p-value <0.001) cell line, respectively (n = 3, t-test). (* = p-value <0.05, ** = p-value <0.01, *** = p-value <0.001)

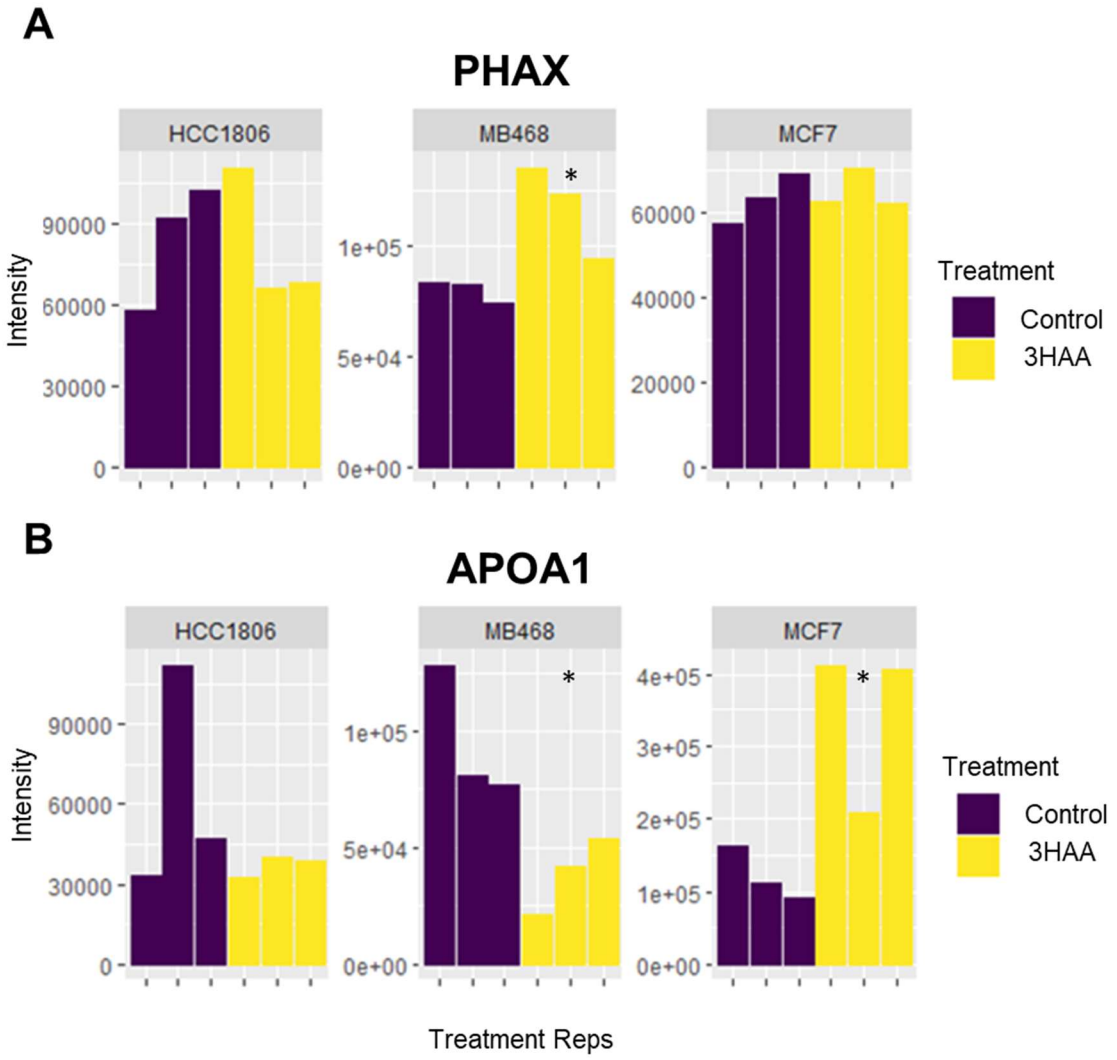

Figure 11. **Proteins matching the molecular function GO terms for significantly up- and down-regulated proteins in MDA-MB-468 cell line across all three cell lines. A**) Protein PHAX matching GO term protein binding for significantly up-regulated proteins. PHAX is significantly up-regulated in the MDA-MB-468 cell line (n = 3, t-test, * = p-value <0.05). **B**) APOA1 protein matching the GO term molecular function, protein binding, for significantly down-regulated proteins. APOA1 is significantly differentially expressed in MCF-7 and MDA-MB-468 (n = 3, t-test, * = p-value <0.05).

DISCUSSION

The mechanism behind the KP enzymes beyond IDO1 are largely unknown. This study aimed to investigate the involvement and function of kynurenine pathway intermediates, downstream of IDO1, in BC metabolism. In this study, the KP was investigated in breast cancer tumour samples and in eight BC cell lines, uncovering the novel finding that KP enzymes such as KYNU are differentially expressed across subsets of tumours and cell lines. The mechanism behind KYNU involvement in breast tumours is poorly understood but previous studies have suggested it functions as a target for hyaluronan (HA) receptor CD44, which has been identified to promote BC metastasis and development (Al-Mansoob et al., 2021).

Additionally, this study showed that KYNU-high tumours were correlated with a high abundance of KP metabolites kynurenic acid (KA) and picolinic acid. KA and picolinic acid are known for having neuroprotective and anticonvulsant properties in the brain, however its role in cancer therapy is not well established (Walczak et al., 2020: Heng e al., 2016). These metabolites have been assessed for their potential anti-tumour activity and studies have found that picolinic acid is involved in immunosuppression by inhibiting effector T cell proliferation (Heng et al., 2016: Hornyák et al., 2018).

To further investigate bioactive role of KP metabolites, we treated eight breast cancer cell lines with four KP metabolites that did not show up in the KYNU high tumours to assess their effect on cell growth. In the present study, the metabolite, 3-HAA, was shown to decrease cell growth in BC cell lines, with the greatest effect on cell growth cell in the MCF-7 cell line. Previous studies investigating KP effects on neurons and astrocytes found that 3-HAA

supplementation significantly decreased neuronal and astroglia NAD+ and increased release of lactate LDH, resulting in cell death (Braidy et al., 2009). In the presence of metals, 3-HAA has also been shown to generate reactive oxygen species (ROS), a cause of DNA damage and apoptosis in immune cells (Heng el al., 2016). 3-HAA has been shown to have a bioactive role in immune-suppression by inducing apoptosis in CD4+ T-cells and encouraging T-cell differentiation towards regulatory T cells rather than anti-tumour T cells (Heng el al., 2016). This metabolite modulates immune functions and limits cytokine-stimulated T cell proliferation (Heng et al., 2016).

Proteomic analysis was performed in attempt to understand 3-HAA mechanism and protein modifications. In doing so, we identified molecular function GO terms corresponding to significant protein differences after treatment with 3-HAA. Go term analysis of significantly differentially expressed proteins in MDA-MB-468 cells revealed over-representation of protein binding activity. The exact mechanism behind this molecular function is not well-established but a downregulation of APOA1, as seen in MDA-MB-468 cells, is consistent with its tumour suppressive role mechanisms (Georgila et al., 2019). Conversely, and consistent with the findings of this study, APOA1 was up-regulated in the MCF-7 cell line and studies have reported APOA1 promotes tumour growth in mouse models of ER-positive BC (Cédo et al., 2016).

Given that the MCF-7 cell growth was most effected by 3-HAA, I have focused the discussion on the biological mechanism of 3-HAA in this cell line. GO term analysis of significantly up-regulated proteins in MCF-7 cells revealed over-representation of leucine transporter, dehydrogenase, and monooxygenase activity. Proteins under the solute carrier family, including SLC3A2 and SLC7A5, match up with the GO term leucine transporter activity. Overexpression of SLC7A5 and SLC3A2 in MCF7 cell lines is consistent with evidence that ER

positive BCs use the amino acid leucine for proliferation (Saito & Soga, 2021). Amino acid transporter SLC7A5 is involved in leucine uptake by ER-positive BC cells, forming a heterodimeric complex with SLC3A2, which is necessary for SLC7A5 activity and substrate specificity (Yan et al., 2019). This suggests that 3-HAA may play a role in leucine depletion in BC cells, which is essential for ER-positive cancer cell growth, but by mechanisms that remain to be explored.

Proteins of the Aldo-keto reductase family including AKR1C1 and AKR1C3 match up with the GO terms including dihydrotestosterone dehydrogenase and monooxygenase activity. Previous studies have found overexpression of AKR1C3 in BC is correlated with ER expression (Jansson et al., 2006). AKR1C3 is a 17β-hydroxysteroid dehydrogenase generating testosterone used to synthesize 17β-estradiol (Penning, 2017). Additionally, AKR1C3 mediated doxorubicin (DOX) resistance has been establish in MCF-7 cells (Zhong et al., 2015). Similarly, to 3-HAA, DOX cytotoxicity has been attributed to the production of reactive oxygen species (ROS) (Zhong et al., 2015). Aldo-keto reductase proteins have been implicated in the resistance of cancer chemotherapeutic agents by eliminating cellular stress from reactive oxygen species (Penning et al., 2021). The proteomics data reveal that 3-HAA effect on cell growth may be related to ER expression in ER-positive cancers.

Conclusion

This study aimed to define the function of KP intermediates in BC cells. To do this, we combined in-vitro cell growth assays, metabolomics, and proteomics. The data suggest a role for kynurenine pathway in BC biology which may reveal metabolic vulnerabilities for BC. Further research is warranted to define the mechanism behind 3-HAA effect on cell growth, but this

study has identified potential involvement of SLC7A5, SLC3A2, AKR1C1, and AKR1C3. Future directions for this study would include performing thermal proteomic profiling (TPP) after treatment with 3-HAA to measure metabolite-protein interactions. Identifying the protein interactions will define the mechanism of action of 3-HAA cell toxicity and decreased cell growth. Additionally, the regulation of KP enzymes besides IDO1 is not well described. Defining how KP enzymes are regulated in BC cells will help define the mechanism of KP up-regulation in cancers.

LITERATURE CITED

Al-Mansoob M, Gupta I, Stefan Rusyniak R, Ouhtit A. 2021. KYNU, a novel potential target that underpins CD44-promoted breast tumour cell invasion. J Cell Mol Med. 25(5):2309-14.

Badawy AA. 2017. Kynurenine pathway of tryptophan metabolism: Regulatory and functional aspects. Int J Tryptophan Res. 2017(10):1178646917691938.

Braidy N, Grant R, Brew BJ, Adams S, Jayasena T, Guillemin GJ. 2009. Effects of kynurenine pathway metabolites on intracellular NAD+ synthesis and cell death in human primary astrocytes and neurons. Int. J. Tryptophan Res: IJTR. 2009(2):61-9.

Cedó L, García-León A, Baila-Rueda L, Santos D, Grijalva V, Martínez-Cignoni MR, Carbó JM, Metso J, López-Vilaró L, Zorzano A, et al. 2016. ApoA-I mimetic administration, but not increased apoA-I-containing HDL, inhibits tumour growth in a mouse model of inherited breast cancer. Sci Rep. 6(1):36387.

Cheang MCU, Chia SK, Voduc D, Gao D, Leung S, Snider J, Watson M, Davies S, Bernard PS, Parker JS, et al. 2009. Ki67 index, HER2 status, and prognosis of patients with luminal B breast cancer. J Natl Cancer I. 101(10):736-50.

Colabroy KL, Begley TP. 2005. Tryptophan catabolism: Identification and characterization of a new degradative pathway. J Bacteriol. 187(22):7866-9.

Fallarino F, Grohmann U, Vacca C, Bianchi R, Orabona C, Spreca A, Fioretti MC, Puccetti P. 2002. T cell apoptosis by tryptophan catabolism. Cell Death Differ. 9(10):1069-77.

Frumento G, Rotondo R, Tonetti M, Damonte G, Benatti U, Ferrara GB. 2002. Tryptophan-derived catabolites are responsible for inhibition of T and natural killer cell proliferation induced by indoleamine 2,3-dioxygenase. J Exp Med. 196(4):459-68.

Ganesh K, Massagué J. 2021. Targeting metastatic cancer. Nature Medicine. 27(1):34-44.

Georgila K, Vyrla D, Drakos E. 2019. Apolipoprotein A-I (ApoA-I), immunity, inflammation and cancer. Cancers. 11(8):1097.

Ghafouri-Fard S, Taherian-Esfahani Z, Dashti S, Kholghi Oskooei V, Taheri M, Samsami M. 2020. Gene expression of indoleamine and tryptophan dioxygenases and three long non-coding RNAs in breast cancer. Exp Mol Pathol. 114:104415.

Girithar H, Staats Pires A, Ahn SB, Guillemin GJ, Gluch L, Heng B. 2023. Involvement of the kynurenine pathway in breast cancer: Updates on clinical research and trials. Br J Cancer.

Hanahan D, Weinberg R. 2011. Hallmarks of cancer: The next generation. Cell. 144(5):646-74.

Heng B, Bilgin AA, Lovejoy DB, Tan VX, Milioli HH, Gluch L, Bustamante S, Sabaretnam T, Moscato P, Lim CK, et al. 2020. Differential kynurenine pathway metabolism in highly metastatic aggressive breast cancer subtypes: Beyond IDO1-induced immunosuppression. Breast Cancer Res. 22(1):113.

Heng B, Lim CK, Lovejoy DB, Bessede A, Gluch L, Guillemin GJ. 2016. Understanding the role of the kynurenine pathway in human breast cancer immunobiology. Oncotarget. 7(6):6506-20.

Hornyák L, Dobos N, Koncz G, Karányi Z, Páll D, Szabó Z, Halmos G, Székvölgyi L. 2018. The role of indoleamine-2,3-dioxygenase in cancer development, diagnostics, and therapy. Front Immunol. 9:151.

Jansson AK, Gunnarsson C, Cohen M, Sivik T, Stål O. 2006. 17beta-hydroxysteroid dehydrogenase 14 affects estradiol levels in breast cancer cells and is a prognostic marker in estrogen receptor-positive breast cancer. Cancer Res (Chicago, Ill.). 66(23):11471-7.

Lai M, Liao C, Tsai N, Chang K, Liu C, Chiu Y, Huang K, Lin C. 2021. Surface expression of kynurenine 3-monooxygenase promotes proliferation and metastasis in triple-negative breast cancers. Cancer Control. 28:10732748211009245.

Lei Zhang, Ovchinnikova O, Jonsson A, Lundberg Am, Berg M, Hansson Gk, Ketelhuth Dfj. 2012. The tryptophan metabolite 3-hydroxyanthranilic acid lowers plasma lipids and decreases atherosclerosis in hypercholesterolaemic mice. Eur Heart J. 33(16):2025-34.

Li J, Van Vranken JG, Pontano Vaites L, Schweppe DK, Huttlin EL, Etienne C, Nandhikonda P, Viner R, Robitaille AM, Thompson AH, et al. 2020. TMTpro reagents: A set of isobaric labeling mass tags enables simultaneous proteome-wide measurements across 16 samples. Nat Methods. 17(4):399-404.

Liu Y, Feng X, Lai J, Yi W, Yang J, Du T, Long X, Zhang Y, Xiao Y. 2019. A novel role of kynureninase in the growth control of breast cancer cells and its relationships with breast cancer. J Cell Mol Med. 23(10):6700-7.

Lu Y, Shao M, Wu T. 2020. Kynurenine-3-monooxygenase: A new direction for the treatment in different diseases. Food Sci Nutr. 8(2):711-9.

Lunt SY, Vander Heiden MG. 2011a. Aerobic glycolysis: Meeting the metabolic requirements of cell proliferation. Annu Rev Cell Dev Bi. 27(1):441-64.

Mishra P, Ambs S. 2015. Metabolic signatures of human breast cancer. Mol Cell Oncol. 2(3):e992217.

Moffett JR, Namboodiri MA. 2003a. Tryptophan and the immune response. Immunol Cell Biol. 81(4):247-65.

Penning TM. 2017. Aldo-keto reductase (AKR) 1C3 inhibitors: A patent review. Expert Opin Ther Pat. 27(12):1329-40.

Penning TM, Jonnalagadda S, Trippier PC, Rižner TL. 2021. Aldo-keto reductases and cancer drug resistance. Pharmacol Rev. 73(3):1150-71.

Saito Y, Soga T. 2021. Amino acid transporters as emerging therapeutic targets in cancer. Cancer Sci. 112(8):2958-65.

Sung H, Ferlay J, Siegel RL, Laversanne M, Soerjomataram I, Jemal A, Bray F. 2021. Global cancer statistics 2020: GLOBOCAN estimates of incidence and mortality worldwide for 36 cancers in 185 countries. CA Cancer J Clin. 71(3):209-49.

Tu R, Ma J, Zhang P, Kang Y, Xiong X, Zhu J, Li M, Zhang C. 2022. The emerging role of deubiquitylating enzymes as therapeutic targets in cancer metabolism. Cancer Cell Int. 22(1):130.

Uhlen M, Zhang C, Lee S, Sjöstedt E, Fagerberg L, Bidkhori G, Benfeitas R, Arif M, Liu Z, Edfors F, et al. 2017. A pathology atlas of the human cancer transcriptome. Science (American Association for the Advancement of Science). 357(6352):660.

Vander Heiden MG, Cantley LC, Thompson CB. 2009. Understanding the warburg effect: The metabolic requirements of cell proliferation. Science. 324(5930):1029-33.

Walczak K, Wnorowski A, Turski WA, Plech T. 2020. Kynurenic acid and cancer: Facts and controversies. Cell Mol Life Sci. 77(8):1531-50.

Wang L, Zhang S, Wang X. 2021. The metabolic mechanisms of breast cancer metastasis. Front Oncol. 10:602416.

Welz B, Bikker R, Junemann J, Christmann M, Neumann K, Weber M, Hoffmeister L, Preuß K, Pich A, Huber R, et al. 2019. Proteome and phosphoproteome analysis in TNF long term-exposed primary human monocytes. Int J Mol Sci. 20(5):1241.

Yan R, Zhao X, Lei J, Zhou Q. 2019. Structure of the human LAT1–4F2hc heteromeric amino acid transporter complex. Nature (London). 568(7750):127-30.

Yeo SK, Guan J. 2017. Breast cancer: Multiple subtypes within a tumor? Trends Cancer. 3(11):753-60.

Zhong T, Xu F, Xu J, Liu L, Chen Y. 2015. Aldo-keto reductase 1C3 (AKR1C3) is associated with the doxorubicin resistance in human breast cancer via PTEN loss. Biomed pharmacother. 69:317-25.